The 2013 World Congress on
Advances in Structural Engineering and Mechanics (ASEM13)
Jeju, Korea, September 8-12, 2013

Dynamic Responses of Floating Platform for Spar-type Offshore Wind Turbine: Numerical and Experimental

*Jin-Rae Cho[1], Yang-Uk Cho[2], Weui-Bong Jeong[3]
Sin-Pyo Hong[3] and Ho-Hwan Chun[3]

[1), 2), 3)] *School of Mechanical Engineering, Pusan National University, Busan 609-735, Korea*
[1)] *jrcho@pusan.ac.kr* & *jrcho@midasit.com*

ABSTRACT

The station keeping and rotational stability are important for spar-type floating offshore wind turbine subject to irregular wind and wave excitations. In this context, this paper addresses the numerical investigation of dynamic response of a spar-type hollow cylindrical floating substructure moored by three mooring lines under irregular wave excitation. The wave-floating substructure and wave-mooring cable interactions are simulated by the coupled BEM-FEM methods in the staggered iterative manner. Through the numerical experiments, the frequency responses of a rigid hollow spar-type floating platform and the mooring cable tension are investigated with respect to the total length and connection position of mooring cables. In order to verify the numerical results, a small-scale prototype (scale: 1/75) of cylindrical floating substructure is experimented in a wave aquatic pool. The comparison of dynamic responses of the floating substructure to one-directional harmonic wave is also presented.

1. INTRODUCTION

In order to secure the dynamic stability of floating-type offshore wind turbine, the station keeping and the rotational vibration control at sea become critical (Tong, 1998). Because of this fundamental requirement, the design of floating-type offshore wind turbine requires extra technologies for floating platform, mooring lines or tension legs, anchors and anticorrosion when compared to fixed-type wind turbine. Floating offshore wind turbines are classified according to how to keep the station position and to control the vertical attitude, such as submerged-, TLP (tension-leg platform)- and spar-types (Lee, 2008; Jonkman, 2009). However, all the types have some things in common from the fact that the station keeping and the vertical attitude are secured by a combination of the buoyancy force, the mooring line tension and additional control device (Colwell and Basu, 2009; Mostafa et al., 2012).

[1)] Vice director of Midas IT.

In case of spar-type floating wind turbine, the buoyancy force produced by a long hollow cylindrical platform supports the whole offshore wind turbine and the tension of mooring lines keeps the station position of spar-type floating substructure. The rotational stability is characterized by the pitch and roll motions of floating substructure, and it is to a large extent obtained by the pitch stiffness of spar-type floating substructure which increases in proportional to the metacetric height (Karimirad et al., 2011). In addition, it is also influenced by both the tension magnitude and the connection position of mooring lines.

The dynamic stability of floating offshore wind turbines subject to wind and wave excitations has been studied by experimentally using scale models (Nielsen et al., 2006; Goopee et al., 2012; Mostafa et at., 2012), by analytically/numerically with the simplified wind turbine geometry and the analytically derived wind/wave loads (Tracy, 2001; Karimirad, 2010; Jensen et al., 2011), or by the combined use of CFD, hydro, FSI (fluid-structure interaction) or/and MBD (multibody dynamics) codes (Zambrano et al., 2006; Jonkman and Musial, 2010; Wang and Sweetman, 2012). Even though the researches on floating offshore wind turbine have been actively conducted, the detailed useful results for the design of spar-type floating platform have not been published yet.

In this context, the current study intends to numerically and experimentally investigate the dynamic response of floating platform and the mooring tension using a 1/75 scale model of 2.5MW spar-type floating wind turbine. Three rotor blades, hub and nacelle are excluded, and three mooring lines are pre-tensioned by means of linear springs. The wave-rigid body interaction simulation of the mooring scale model is performed by the coupled BEM-FEM method. As well, the scale model is manufactured and experimented in wave tank by means of the specially designed sensor and data acquisition system. The response amplitude operators (RAO) of the scale model and the mooring tensions are obtained and compared.

2. SPAR PLATFORM FOR FLOATING OFFSHORE WIND TURBINE

The most important requirement of renewable energies is the efficiency and capacity, and in this regard wind power draws an intensive attention thanks to its potential to generate a huge amount of electricity from plenty of winds around us (Hansen and Hansen, 2007). Wind turbines in the early stage were designed for the installation on the ground and showed the rapid increase in both the total installation number and the maximum power generation capacity. However, this worldwide trend encountered several obstacles such as the infringement of living environment and the limitation of being high-capacity and making large wind farm. This critical situation naturally turned the attention to the offshore sites, a less restrictive installation place.

Offshore wind turbines are classified largely into two categories, fixed- and floating-type according to how the wind turbine tower is supported. Differing from the fixed-type, the floating-type wind turbine is under the concept design stage because several core technologies are not fully settled down (Karimirad et al., 2011). In particular, the design of floating substructure becomes a critical subject because it supports the entire wind turbine system and influences the dynamic stability. Currently, three types of floating substructures are considered, barge, tension leg (TLP) and spar types.

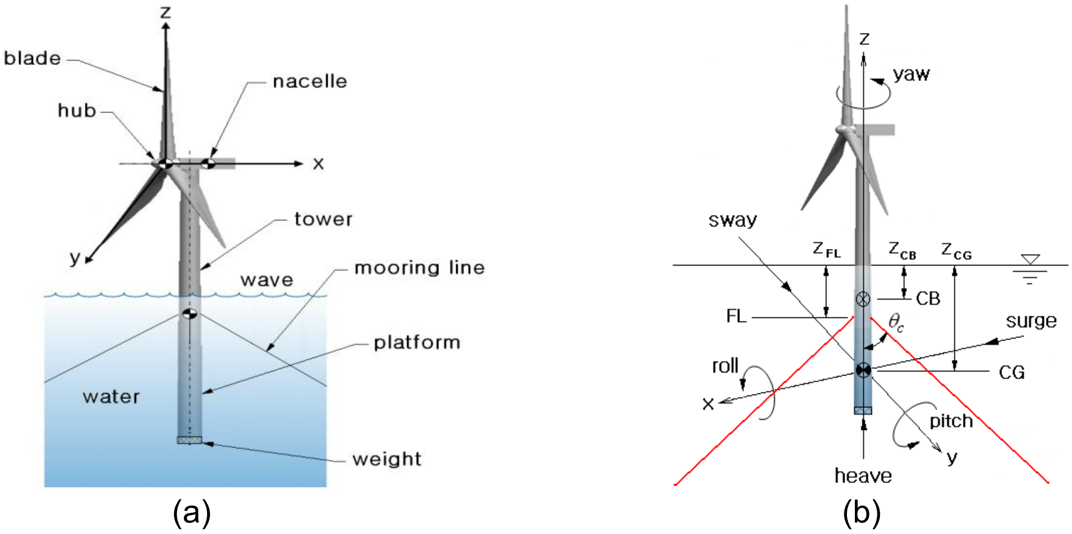

Fig. 1 (a) Spar-type floating offshore wind turbine, (b) 6-DOF rigid body motions.

A typical spar-type floating offshore wind turbine is represented in Fig. 1, where the entire wind turbine is supported by the buoyancy force and the vertical position is adjusted by the weight at the bottom of platform. The dynamic displacement of wind turbine which is caused by wind, wave and current loads is restricted by the tension of mooring lines (Lefebvre and Collu, 2012). The dynamic stability of floating-type wind turbine is evaluated in terms of three translation (i.e., surge, sway and heave) and three rotation motions (i.e., pitch, roll and yaw). These six degrees of freedom are coupled to each other, and the pitch angle is the most significant parameter to evaluate the dynamic stability of wind turbine.

The rigid body translational motions are characterized by the stiffness and fairlead angle θ_c of mooring cables as well as the total mass of floating platform. The stiffness and fairlead angle are in turn influenced by the specific weight and total length of mooring cables. Meanwhile, the rigid body rotational motions are influenced by the stiffness itself of floating platform and the fair lead position Z_{FL} and angle θ_c. The stiffness of floating platform to the pitch and roll motions is known to be proportional to the relative vertical distance $(Z_{CB} - Z_{CG})$ between the centers of buoyancy and gravity (Karimirad et al., 2011) as well as the mass moments of platform.

3. RIGID BODY-FLUID INTERACTION

Referring to Fig. 3(a), let us $\Omega_F \in \Re^3$ be a semi-infinite unbounded flow domain with the boundary $\partial\Omega_F = \overline{S_F \cup S_B \cup \Gamma_I}$ and denote $\boldsymbol{V}$ be a continuous triple-vector water velocity field, where S_F, S_B and Γ_I indicate the free surface, seabed and flow-structure interface respectively. Water is assumed to be inviscid and incompressible and water flow is irrotational so that there exists a velocity potential function $\phi(\boldsymbol{x};t)$ satisfying $\phi(\boldsymbol{x};t):\boldsymbol{V} = \nabla\phi$. Then, the flow field is governed by the continuity equation

$$\nabla^2\phi = 0, \quad in \quad \Omega_F \times (0, \hat{t}] \tag{1}$$

and the boundary conditions given by

$$\frac{\partial \phi}{\partial n} = \dot{\boldsymbol{u}} \cdot \boldsymbol{n}, \quad on \quad \Gamma_I \tag{2}$$

$$g\frac{\partial \phi}{\partial z} + \frac{\partial^2 \phi}{\partial t^2} = 0, \quad on \quad S_F \tag{3}$$

$$\frac{\partial \phi}{\partial z} = 0, \quad on \quad S_B \tag{4}$$

with $\hat{t}$ being the time period of observation, g the gravity acceleration, $\boldsymbol{n}$ the outward unit vector normal to the structure boundary. In addition, the potential function satisfies the radiation condition: $\phi \to 0$ as $r \to \infty$ at the far field.

The substructure occupying the material domain $\Omega_S \in \Re^3$ with the boundary $\partial\Omega_S = \overline{\Gamma_D \cup \Gamma_N \cup \Gamma_I}$ is assumed to be a rigid body. By denoting $\{\boldsymbol{d}, \theta\}$ be its rigid body translation and rotation at the center of mass, the dynamic motion of the substructure is governed by the conservation of linear and angular momentums

$$m\ddot{\boldsymbol{d}} + c\dot{\boldsymbol{d}} + k\boldsymbol{d} = \boldsymbol{F}, \quad in \quad \Omega_S \times (0, \hat{t}] \tag{5}$$

$$\boldsymbol{I}_\theta \ddot{\theta} + c_\theta \dot{\theta} + k_\theta \theta = \boldsymbol{M}, \quad in \quad \Omega_S \times (0, \hat{t}] \tag{6}$$

and the initial conditions given by

$$\{\dot{\boldsymbol{d}}, \dot{\theta}\}_{t=0} = \{\dot{\boldsymbol{d}}, \dot{\theta}_0\}, \quad \{\boldsymbol{d}, \theta\}_{t=0} = \{\boldsymbol{d}_0, \theta_0\} \tag{7}$$

In which m, c, k, c_θ and k_θ denote the total mass and the damping and stiffness coefficients for the translational and rotational degrees of freedom, respectively. Meanwhile, $\boldsymbol{I}_\theta$ indicates the matrix of mass moments of inertia with respect to the center of mass, and $\boldsymbol{F}$ and $\boldsymbol{M}$ are the external force and moment vectors which are calculated by

$$\boldsymbol{F} = \int_{\Gamma_I} p\boldsymbol{n}\, ds, \qquad \boldsymbol{M} = \int_{\Gamma_I} p\boldsymbol{r} \times \boldsymbol{n}\, ds \tag{8}$$

Here, p and $\boldsymbol{r}$ are the hydrodynamic pressure and the position vector from the center of mass, respectively.

Meanwhile, catenary mooring cable of length L is a slender flexible structure subject to hydrodynamic pressure, self weight, inertia force and drag force. Referring to Fig. 3(b), the nonlinear differential equations of motion (Goodman and Breslin, 1976; Aamo and Fossen, 2000) for the differential cable element $d\ell$ are governed by the equilibrium equations in translation and rotation,

$$(m_c + m_a)\frac{\partial \dot{\boldsymbol{u}}_c}{\partial t} = \frac{\partial \boldsymbol{T}_c}{\partial s} + (1+\gamma)\boldsymbol{F_c} \tag{9}$$

$$\frac{\partial \boldsymbol{M_c}}{\partial s} = -\boldsymbol{r_t} \times (1+\gamma)\boldsymbol{T_c} \tag{10}$$

with the boundary conditions given by

$$\dot{\boldsymbol{u}}_c = 0, \quad \theta_c = \theta_c^B \quad at \quad s = 0\,(at\ seabed) \tag{11}$$

$$\dot{\boldsymbol{u}}_c = \dot{\boldsymbol{d}}_P, \quad \theta_c = \theta_c^P \quad at \quad s = L\,(at\ connecting\ point) \tag{12}$$

In which, m_c indicates the mass per unit arc length, m_a the added mass of water, $\dot{\boldsymbol{u}}_c$ the velocity vector, s the arc length of unstressed cable, and γ the engineering strain. In addition, $\boldsymbol{r}_t$ is the vector tangent to the cable center line, $\boldsymbol{M}_c$ the resultant internal moment, and $\boldsymbol{F}_c$ the external loading per unit arc length due to the self weight $\rho_c g$, and $\boldsymbol{F}_n$, $\boldsymbol{F}_\tau$ and $\boldsymbol{F}_q$ the normal, tangential and binormal drag forces (Morison et al., 1950).

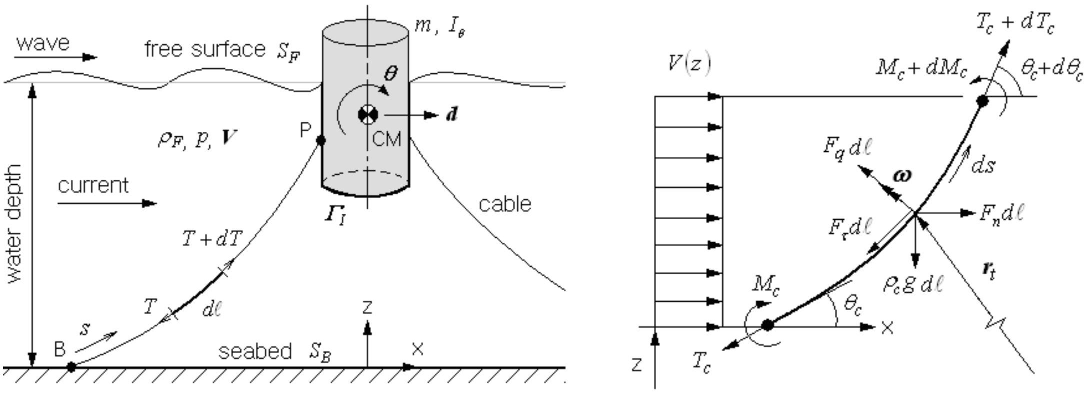

(a) (b)

Fig. 2 (a) A rigid floating body moored by catenary cables in irregular wave (b) forces acting on the cable element.

The potential flow is interpolated by the boundary element method while the dynamic motions of the rigid floating substructure and mooring cables are approximated by the finite element method. The Euler-Lagrange coupling method is employed to deal with the interaction between the rigid body structure motion and the water flow, and it with the lapse of time is numerically implemented in a staggered iterative manner (Sigrist and Abouri, 2006; Cho et. al., 2008).

4. NUMERICAL EXPERIMENTS

A simplified 75:1 scale model of $2.5MW$ spar-type floating offshore wind turbine with three equal catenary mooring cables is taken for investigating the dynamic response of the cylindrical floating platform and mooring cables. The geometry dimensions, masses and moments of inertia of the major components are given in Fig. 3(a) and Table 1. Three rotor blades, hub and nacelle assembly are simplified as a lumped mass for both the numerical simulation and the wave tank experiment. The center of buoyancy (CB) and the center of mass (CM) are measured from the bottom of platform and the relative vertical distance between two centers is set by $10.0m$.

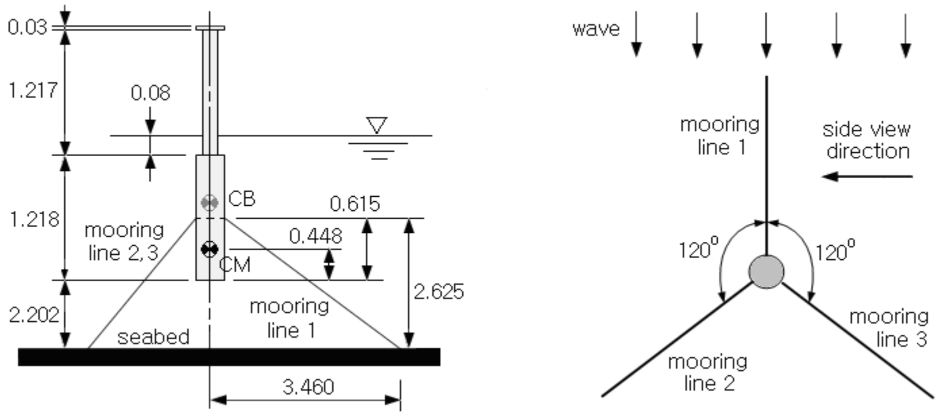

Fig. 3 A simplified spar-type platform moored by three nylon cables (unit: m)

The width and depth of the water pool are set by $8\times100m$ and the height from seabed is set by $35m$, respectively. The total length of each mooring line and the relative angles between two adjacent mooring lines are set by $4.343m$ and 120^o respectively, and three mooring lines are equally pre-tensioned by $0.49kgf$. The cross sectional area A_c, the mass per unit length γ_c, the stiffness EA and the maximum allowable tension T_c^{max} are $0.02m^2$, $90kg/m$, $1.0\times10^9 N$ and $1.0\times10^7 N$ respectively, and the hydrodynamic drag coefficient C_D is set by 0.025. Three mooring lines are aligned such that mooring line 1 opposites to the incoming direction of one-dimensional regular harmonic wave as represented in Fig. 3(a), and the amplitude and frequency of regular harmonic wave are set by $1.0m$ and $0.01\sim0.5Hz$, respectively.

Table 1. Major specifications of scale platform model.

Components	Items	Values
Platform	Diameter (upper & lower)	$0.076m$, $0.150m$
	Thickness (upper & lower)	$2.9m$, $3.2m$
	Moments of inertia (pitch, roll & yaw)	$9.240kg\cdot m^2$, $9.237kg\cdot m^2$ $0.065kg\cdot m^2$

Figs. 4 and 5 represented the simplified scale platform model and the wave tank with the dimensions of $100m$ in length, $8m$ in width, and $3.5m$ in depth. On the right side of the wave tank, three cameras for the vision system and a data acquisition system are placed. The scale platform model is moored by three nylon mooring lines, and tension sensors and springs are connected between mooring lines and fairleads. A square plate is installed on the top of platform, where infrared light emit diodes (LEDs) are attached to measure the dynamic motion of platform. The light signals of LEDs are detected by a trinocular vision system, and the six rigid body motions of the floating platform are monitored. In addition, a small-size attitude and heading reference system (AHRS) manufactured by Micro-Electro-Mechanical-Systems (MEMS) Technology is attached on the top of platform to measure the acceleration, angular velocity, and attitude of the floating platform. The sensor sends the motion signals to the computer through USB (universal serial bus) port in RS-232 protocol.

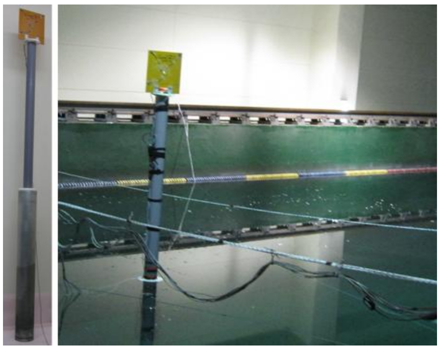

(a)

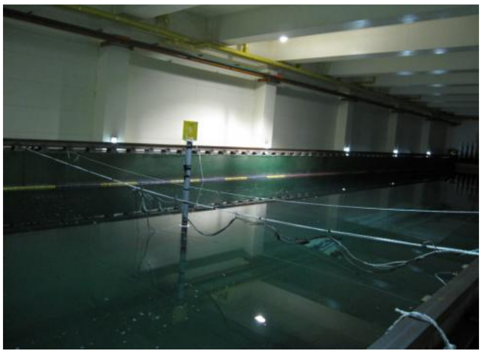

(b)

Fig. 4. Experimental setup for obtaining the dynamic response of the moored scale model: (a) scale model (b) one-directional wave tank.

The response operators (RAOs) of surge, heave and pitch motions obtained by simulation and experiment are compared in Fig. 5. It is observed that the resonance frequencies predicted by simulation are in excellent agreement with the experiment. Furthermore, it is verified that the pitch amplitudes between simulation and experiment are in good agreement over all frequency range. But, the amplitudes in surge and heave motions which are predicted by simulation show the discrepancy. It is because the damping effect is not appropriately reflected into the numerical simulation.

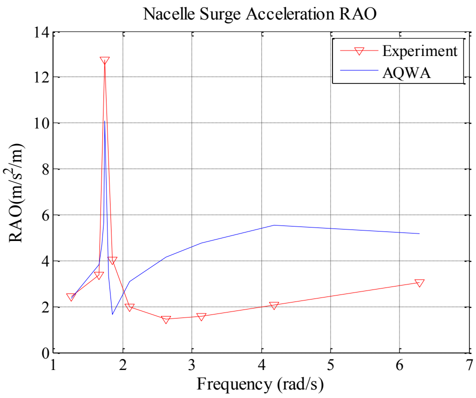

(a)

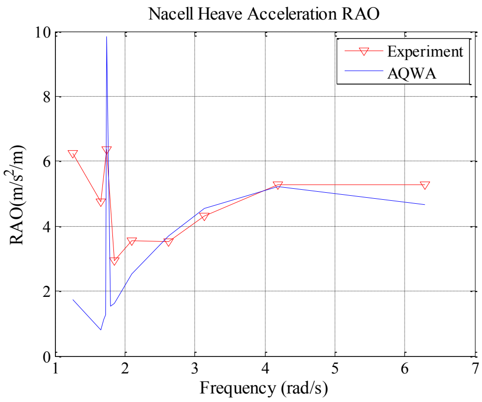

(b)

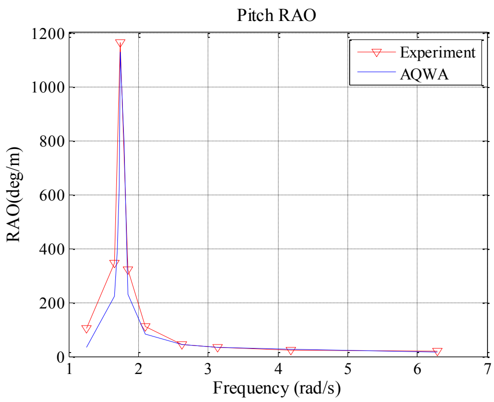

(c)

Fig. 5. Response amplitude operators (RAOs): (a) surge, (b) heave, (c) pitch.

CONCLUSION

Dynamic response of spar-type floating platform has been investigated by numerical and experimental methods using a 1/75 scale model by excluding the detailed upper part. The numerical simulation of the rigid body-fluid interaction was carried out by a staggered iterative BEM-FEM method, while the experiment was performed in a wave tank using a specially designed vision and data acquisition system. Through the comparison of the response amplitude operators (RAO) of surge, heave and pitch motion to regular harmonic wave, it has been verified that the numerical results are in a good agreement with the experiment.

ACKNOWLEDGEMENT

This work was supported by the Human Resources Development of the Korea Institute of Energy Technology Evaluation and Planning (KETEP) grant funded by the Korea Ministry of Knowledge Economy (No. 20114030200070).

REFERENCES

Aamo, O.M., Fossen, T.I. (2000) “Finite element modeling of mooring lines,” *Mathematics of Computers in Simulation* **53**(4-6):415-422.

Cho, J.R., Park, S.W., Kim, H.S., Rashed, S. (2008) “Hydroelastic analysis of insulation containment of LNG carrier by global-local approach,” *International Journal for Numerical Methods in Engineering* **76**:749-774.

Colwell, S., Basu, B. (2009) “Tuned liquid column dampers in offshore wind turbines for structural control,” *Engineering Structures* **31**:358-368.

Goodman, T.R., Breslin, J.P. (1976) “Statics and dynamics of anchoring cables in waves,” *Journal of Hydronaut* **10**(4):113-120.

Goopee, A..J., Koo, B..J., Lambrakos, K.F., Kimball, R.W. (2012) “Model tests for three floating wind turbine concepts,” *Proceedings of Offshore Technology Conference*, Houston, USA.

Hansen, A.D., Hansen, L.H. (2007) ”Wind turbine concept market penetration over 10 years (1995-2004),” *Wind Energy* **10**:81-97.

Jensen, J., Olsen, A., Mansour, A. (2011) “Extreme wave and wind response predictions,” *Ocean Engineering* **38**:2244-2253.

Jonkman, J. (2009) “Dynamics of offshore floating wind turbines-model development and verification,” *Wind Energy* **12**:459-492.

Jonkman, J., Musial, W. (2010) “Offshore code comparison collaboration (OC3) for IEA task 23 offshore wind technology and development,” *Technical Report NREL/TP-5000-48191*, Colorado.

Karimirad, M. (2010) “Dynamic response of floating wind turbines,” *Transaction B: Mechanical Engineering* **17**(2):146-156.

Karimirad, M., Meissonnier, Q., Gao, Z., Moan, T. (2011) “Hydroelastic code-to-code comparison for a tension leg spar-type floating wind turbine,” *Marine Structures* **24**:412-435.

Lee, S.H. (2008) *Dynamic Response Analysis of Spar Buoy Floating Wind Turbine Systems*, Ph.D. Thesis, MIT.

Lee, H.H., Wong, S.H., Lee, R.S. (2006) “Response mitigation on the offshore floating platform system with tuned liquid column damper,” *Ocean Engineering* **33**:1118-1142.

Lefebvre, S., Collu, M. (2012) “Preliminary design of a floating support structure for a 5MW offshore wind turbine,” *Ocean Engineering* **40**:15-26.

Morison, J.R., O’Brien, M.P., Johnson, J.W., Schaaf, S.A. (1950) “The force exerted by surface waves on piles,” *Petroleum Transaction* **189**:149-157.

Mostafa, M., Murai, M., Nishimura, R., Fujita, O., Nihei, Y. (2012) “Experimental valdation for motion of spar-type floating wind turbine at inclination with effect of gyro moment of the rotating blade of windmill,” *International Offshore and Polar Engineering Conference*, Rhodes, Greece.

Nielsen, F.G., Hanson, T.D., Skaare, B. (2006) “Integrated dynamic analysis of floating offshore wind turbines,” *Proceedings of 25th International Conference on Offshore Mechanics and Arctiv Engineering (OMAE2006)* **1**:671-679.

Sigrist, J.F., Abouri, D. (2006) “Numerical simulation of a non-linear coupled fluid-structure problem with implicit and explicit coupling procedure,” *Proceedings of ASME Pressure Vessel and Piping Division Conference*, Vancouver, Canada, 23-27.

Tong, K.C. (1998) “Technical and economic aspects of a floating offshore wind farm,” *Journal of Wind Engineering and Industrial Aerodynamics* **74-76**:399-410.

Tracy, C. (2007) *Parametric Design of Floating Wind Turbines*, Maters Thesis, MIT.

Wang, L., Sweetman, B. (2012) “Simulation of large-amplitude motion of floating wind turbines using conservation of momentum,” *Ocean Engineering* **42**:155-164.

Zambrano, T., MacCready, T., Kiceniuk, T., Goddier, D.G., Cermelli, C.A. (2006) “Dynamic modeling of deepwater offshore wind turbine structures in gulf of Mexico storm conditions,” *Proceedings of 25th International Conference on Offshore Mechanics and Arctic Engineering*, Hamburg, Germany.